Polyhedron 52 (2013) 1299–1305

Contents lists available at SciVerse ScienceDirect

Polyhedron

journal homepage: www.elsevier.com/locate/poly

A computational perspective on magnetic coupling, magneto-structural correlations and magneto-caloric effect of a ferromagnetically coupled {Gd^{III}–Gd^{III}} Pair

Thayalan Rajeshkumar, Saurabh Kumar Singh, Gopalan Rajaraman *

Department of Chemistry, Indian Institute of Technology – Bombay, Powai, Mumbai 400076, India

ARTICLE INFO

Article history:
Available online 28 June 2012

Dedicated to Alfred Werner on the 100th Anniversary of his Nobel Prize in Chemistry in 1913.

Keywords:
SMMs
MCE
DFT calculations
Magnetic coupling in {4f–4f}
{Gd^{III}–Gd^{III}} pair
Magneto-structural correlations

ABSTRACT

Density functional calculations have been performed on a dinuclear {Gd^{III}–Gd^{III}} complex [{Gd(OAc)$_3$(H$_2$O)$_2$}$_2$]·4H$_2$O (**1**) which has recently been reported to have a very large MCE [M. Evangelisti, O. Roubeau, E. Palacios, A. Camon, T.N. Hooper, E.K. Brechin, J.J. Alonso, Angew. Chem., Int. Ed. 50 (2011) 6606]. The focus here is (i) to asses a suitable functional within DFT framework to compute good numerical estimate of *J* values (ii) to probe the mechanism of coupling between the two Gd^{III} ions via computational means (iii) to develop magneto-structural correlations to relate the sign and strength of *J* to specific structural parameter and (iv) to conceive the origin of large magneto-caloric effect (MCE) observed. Testing a series of functionals and a set of basis sets, it is evident that the hybrid B3LYP functional behaves marginally well over others with a combination of SARC basis set incorporating ZORA (zeroth-order regular approximation) relativistic effect for the Gd^{III} ions. The MO and NBO tools have been utilized to probe the mechanism of coupling and this reveals that there are two contributions. The first is charge transfer in nature leading to a ferromagnetic contribution due to the involvement of empty 6s/5d/6p orbitals of Gd^{III} ions and the second contribution is due to 4f–4f orbital overlap and this adds to both ferro and antiferromagnetic part of the exchange. In **1**, the ferromagnetic contribution prevails over the other leading to a net ferromagnetic *J*. The developed magneto-structural correlations reveal that the Gd–O–Gd angle is an important parameter as it switches the coupling from ferro to antiferro at lower angles. A weak intermolecular ferromagnetic interaction mediating via H-bonding interaction results in a ferromagnetic interaction at low temperatures and hence a large MCE.

1. Introduction

There is a large interest in the studies of polynuclear clusters of paramagnetic ions in recent years due to their connection to nanotechnology and the related applications [1–4]. These nano-structured paramagnetic clusters are collectively known today as molecular nano magnets (MNMs). The MNMs are further classified into several types such as – single molecule magnets (SMMs) [1,2,5–7], single chain magnets (SCMs) [8], single ion magnets (SIMs) [9] and antiferromagnetic wheels to name a few [10]. They have wide range of potential applications varying from information storage devices [1,2], molecular spintronics [3] to Q-bits in quantum computing [4]. In this area, lanthanide compounds occupy a distinct position as they satisfy many physical properties that the potential applications demands such as large intrinsic anisotropy (SMMs), weak exchange interaction (MCE), quantum tunneling of magnetization (quantum computing). This is manifested by the recent discoveries such as mononuclear lanthanide complexes exhibiting slow relaxation of magnetization [5–10] and polynuclear lanthanide complexes holding record barrier height for the magnetization reversal. A recent list of breakthrough includes {Dy^{III}_4}, {Dy^{III}_5} and {Dy^{III}_6} clusters [11] with record barrier height of 170, 530 and 230 K.

Apart from the potential applications mentioned above one of the promising application that emerges in recent years is the molecular refrigerant [12]. This gains much attention because of the possibility of replacing the highly expensive and rare helium-3 in ultralow-temperature applications [13]. These molecular refrigerants are environmentally friendly and are working on the principle of magnetic caloric effect (MCE) [14]. The MCE is basically related to the change in entropy (ΔS) during adiabatic demagnetization with change in applied magnetic field [15]. The primary condition to have large MCE is to have a large isotropic spin (*S*) ground state and weak magnetic interactions. There are a few 4f-based clusters reported to be a potent magnetic coolers [16] working on the principle of MCE. The Gd^{III} is an ideal candidate for designing the magnetic coolers as it possess the largest possible monomeric spin ($S = 7/2$) and is isotropic in nature. Besides being a 4f-ion it mediates a weak coupling – thus fulfilling all the prerequisite of achieving a large MCE. This is evident from the fact that there are several Gd^{III} based polynuclear clusters reported so far

* Corresponding author. Tel.: +91 22 2576 7183; fax: +91 22 2576 7152.
E-mail address: rajaraman@chem.iitb.ac.in (G. Rajaraman).

0277-5387/$ - see front matter © 2012 Elsevier Ltd. All rights reserved.
http://dx.doi.org/10.1016/j.poly.2012.06.017

possessing a very large MCE [16–22]. Recent breakthrough in this field includes a binuclear Gd^{III} complex [16] exhibiting a very large MCE with ΔS of -40 J kg^{-1} K^{-1}.

The synthesis of new generation magnetic coolants requires a thorough understanding and control of the microscopic spin Hamiltonian parameters. In this regard, computational tools are indispensable – both in calculating the spin Hamiltonian parameters as well as in predicting the magnetic properties of the paramagnetic complexes [23–26]. The DFT calculations carried out by us [27] and others [28] previously on {3d–4f} system reveals the robustness in predicting the sign as well as the strength of the exchange interaction.

Here we have chosen two dinuclear gadolinium complexes, $[\{Gd(OAc)_3(H_2O)_2\}_2]\cdot 4H_2O$ (**1**) [16] and $[\{Gd(OAc)_3(H_2O)_2\}_2]\cdot 2H_2O$ (**2**) [29]. The primary focus will be complex **1** where DFT computation has been performed to asses a suitable functional to calculate the magnetic coupling in $\{Gd^{III}$–$Gd^{III}\}$ pair, to understand the mechanism of magnetic coupling in $\{Gd^{III}$–$Gd^{III}\}$ pair and to develop the magneto-structural correlations for the $\{Gd^{III}$–$Gd^{III}\}$ pair. Apart from computing the intramolecular exchange interaction, we have also computed the intermolecular exchange which propagates through H-bonding interaction between two $\{Gd^{III}{}_2\}$ dimeric units. The calculation on complex **2** has been performed essentially for comparative purpose and also to evaluate the goodness of density functional methodology employed.

2. Computational details

The magnetic exchange has been obtained using the following spin Hamiltonian which includes spins of two gadolinium atoms (S_{Gd1} and S_{Gd2}) where S_{Gd1} and S_{Gd2} are the spin on Gd^{III} ions.

$$\hat{H} = -J \cdot S_{Gd1} \cdot S_{Gd2}$$

In the above equation, J represents isotropic exchange coupling constant and its value has been calculated using DFT and Broken symmetry approach [30]. The BS method has proven record of yielding good numerical estimate of J constants for a variety of complexes [23–27,30,31]. A detailed technical discussion on computational details on the J values using broken symmetry approach on dinuclear as well as polynuclear complexes have been reported elsewhere [23–28]. We performed most of our calculations using G09 suite of program [32] with fragment approach employing hybrid B3LYP functional [33] along with triple zeta basis set for C, H, and O atoms along with that Cundari–Stevens (CS) relativistic effective core potential on gadolinium atoms (level I) [34]. We have also performed calculations with all electron basis set for comparison using ORCA suite of programs [35] employing SARC [36] on Gd, along with their Ahlrichs SVP basis set on rest of the elements [37]. These calculations have been performed by incorporating relativistic effects either via the ZORA [38] or via DKH (Douglas–Kroll–Hess) methods [39,40] (level II). A very tight SCF convergence has been employed throughout.

3. Result and discussion

3.1. Exchange interaction in dinuclear Gd^{III} complex

We have carried out DFT studies on two gadolinium complexes **1** (see Fig. 1a) and **2**. Although the coordination environment is same for both the complexes, due to the difference in the number of water molecules in the second coordination sphere [41], there are some small structural changes and this leads to a different J value. In both the complexes, the Gd^{III} atoms are linked by two chelating carboxylate bridges. For **1**, the distance between Gd^{III} ions is 4.183 Å. The bridging Gd–O distances are found to be asymmetric with the value of 2.558 and 2.393 Å. The Gd–O–Gd angle is found to be 115.3° with the Gd–O–Gd–O dihedral angle of 0°. The DFT calculations (level I) yield the J value of 0.03 cm^{-1} which is in good agreement to the experimental J value of 0.06 cm^{-1}. For complex **2**, the DFT calculated J value is found to be 0.04 cm^{-1} is also in agreement to the experimental J value of 0.03 cm^{-1}. The difference in the magnitude of the J value between **1** and **2** are related to small difference in the Gd–O–Gd angle (vide infra).

In spite of its simple structure, the enormous MCE found in **1** made us curious to look into the exchange pathways. The magnetic exchange in **1** propagates through two μ_2 fashioned carboxylate bridges (η^2:η^1 mode) and two hydrogen bonding interactions between the coordinated water and the carboxylates. In order to understand the magnitude of exchange propagating through hydrogen bonding, we have designed a model complex where water molecules are rotated to avoid the H-bonding interactions. The calculated J value in this model complex is found to be 0.03 cm^{-1} disclosing the fact that the contribution due to internal H-bonding is negligible.

3.2. Method assessment

Although a method assessment is available for the evaluation of magnetic exchange interaction in transition metal compounds [23] and in {3d–4f} complexes [27], no suitable functional or basis set are advocated for a {4f–4f} pair coupling. Previously spin density functional calculations using a pure BLYP functional and small core TZ2P basis including ZORA relativistic effect has been performed to evaluate the magnetic coupling in some dinuclear and hexanuclear Gd^{III} compounds [42]. Although good numerical estimates have been obtained [23–27], a pure functional of this type has been found to predict a wrong sign of J for a {3d–4f} pair [43–45]. This necessitates the compulsion for a comprehensive method assessment for a {4f–4f} pair and this has been our initial focus. We have tested several hybrid as well as non hybrid functionals with a variety of local and exchange correlations to assess a suitable functional for the computation of J in {4f–4f} based systems. The computed results are summarized in Table 1. With B3LYP functional, three different basis set combinations have been tested with the first one treating the relativistic effects via effective core potential (ECP) and secondly with DKH and ZORA. Our calculations clearly reveals that there is a strong basis set dependency with SARC basis set for Gd^{III} with ZORA yielding the best estimate of the J value for **1**. The functional tests have been performed only with the ECP/DKH relativistic basis set (see ESI for details). The functionals tested here, apart from the functional form also differ in the percentage of HF exchange contribution [33,46–50]. Despite these differences, it is clear from the Table 1 that all the tested functionals are yielding J values which are in agreement to the experimental results. Since there is no significant advantage of employing a pure functional for the evaluation of J values [42], we would continue to employ the popular B3LYP functional for the further studies.

3.3. Mechanism of coupling

To explore the reasons behind the ferromagnetic exchange in **1**, MO and NBO analysis have been performed. The Kahn-Brait model [51] which relates the overlap between non-orthogonal orbitals to the nature of exchange interaction can be employed to understand the individual contribution to the net exchange interaction J. The J value has contributions from both J_F (ferromagnetic part of J) and J_{AF} (antiferromagnetic part of J) parts and the sign of exchange is decided by the dominating factor. The spin density plots can help us to probe the electronic origin of exchange. The spin densities on two Gd^{III} ions are found to be 7.027 (similar values) and larger

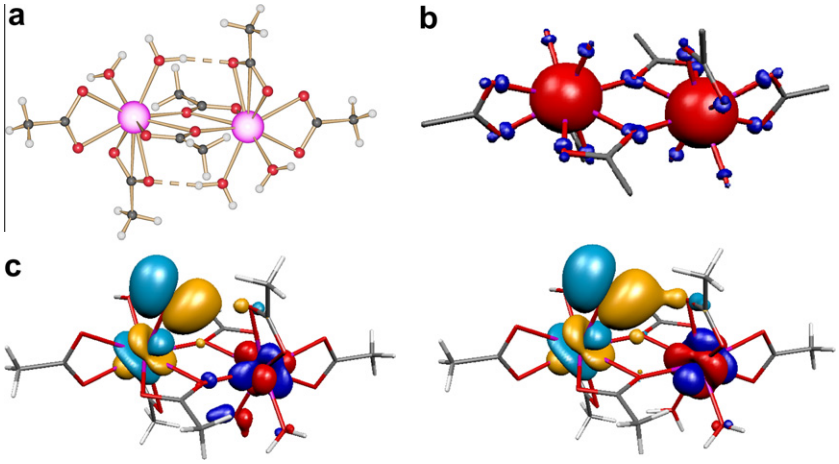

Fig. 1. Colour scheme: Gd^{III} in pink, oxygen in red, carbon in black, hydrogen in white. (a) Crystal structure of complex **1**. (b) DFT computed spin density plot for the $S = 7$ ground state with the red and blue region indicating positive and negative spin densities respectively. (c) The two representative f-orbitals (α spin on left and β on right) which shows the strongest overlap. The isodensity surface represented which corresponds to a value of 0.015 $e^-/bohr^3$. (Color online.)

Table 1
DFT computed J values using different functionals.

Functional	J (cm^{-1})	Gd^{III} spin densities (HS)	Percentage of HF exchange (%)	Basis set	Relativistic
Exp	0.06				
B3LYP	0.03	(7.027, 7.027)	20	Gd (CSDZ), and others (TZV)	ECP
B3LYP	0.04	(7.026, 7.026)	20	Gd (SARC), and others(TZV)	DKH
B3LYP	0.05	(7.031, 7.031)	20	Gd (SARC), and others(TZV)	ZORA
X3LYP	0.03	(7.027, 7.027)	21.8	Gd (CSDZ), C, H, O (TZV)	ECP
BLYP	0.03	(7.021, 7.021)	0	Gd (CSDZ), C, H, O (TZV)	ECP
BP86	0.03	(7.031, 7.031)	0	Gd (CSDZ), C, H, O (TZV)	ECP
TPSSh	0.04	(7.051, 7.051)	10	Gd (CSDZ), C, H, O (TZV)	ECP
TPSS0	0.05	(7.050, 7.050)	25	Gd (SARC), and others(TZV)	ZORA
PW91	0.002	(7.020, 7.020)	0	Gd (SARC), and others(TZV)	ZORA
OLYP	0.001	(7.014, 7.014)	0	Gd (SARC), and others(TZV)	ZORA

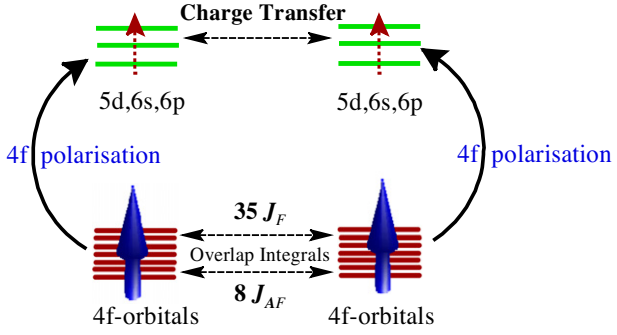

Fig. 2. Schematic mechanism proposed for magnetic coupling in {Gd^{III}–Gd^{III}} pair.

value than what is expected suggests that spin polarization mechanism is operational. From the spin density plot (see Fig. 1b) and negative spin density values (see ESI Table S3) one can infer that due to the contracted nature of the 4f-orbitals in the Gd^{III} ion, the spin delocalization is so poor that it is exceeded by the spin polarization, leading to opposite spin densities on the atoms around the Gd atom. The bridging oxygens are having more spin densities than other oxygens due to the fact that they are polarized by both the Gd^{III} atoms and this polarization essentially favors a ferromagnetic coupling as per the McConnell mechanism [52].[1] A schematic mechanism developed using our analysis is shown in Fig. 2.

The computation of overlap integrals between the singly occupied magnetic orbitals offers insight into the J_{AF} contribution to the total exchange whereas the J_F contribution can be perceived from the charge transfer to the vacant d-orbitals using NBO analysis. Since the molecule does not possess any crystallographic symmetry, in principle there are 49 interactions. Computing all these interactions reveals that, there are six significant overlap between a 4f orbital of Gd(1) (α) and another 4f orbital of Gd(2) (β) (see Fig. 3 for a representative set). Besides there are also some moderate overlap detected for another eight pairs (see ESI Table S4). Thus, all these fourteen interactions are likely to contribute to J_{AF} while the rest of the 35 interactions are orthogonal and are likely to contribute to J_F. Since the number of J_F is dominating, it is natural to expect that the net exchange to be ferromagnetic in nature. In addition, the empty 5d/6s/6p orbitals of the Gd^{III} can also play a vital role in magnetic coupling. These additional contributions are likely to add to the J_F part of the exchange. The NBO analysis indicates that the formally empty 5d/6s/6p orbitals of Gd^{III} have significant occupation (0.73/0.19/0.37). These empty orbitals gain occupation primarily via polarization of the 4f-orbitals. Besides, the NBO second order perturbation analysis reveals a significant donor–acceptor contribution between two Gd^{III} atoms where a d–p mixed ($Gd^{III}(6p_x$)–$Gd^{III}(5d_{x^2-y^2}$)) orbital donates electrons from Gd(1) to the d–s mixed ($Gd^{III}(6s)$–$Gd^{III}(5d_{xy})$) orbital of Gd(2) and vice versa. The stabilization energy for this interaction is 23.4 kcal/mol and this highlights the significance of this interaction (see Fig. 3 for a representative donor–acceptor NBO orbital).

[1] Note here that spin polarization is not the sole mechanism which decides the sign of coupling. A study on magnetic coupling in Cu(II) complex suggest that spin polarization is not directly related to the ferromagnetic coupling see Ref. [55].

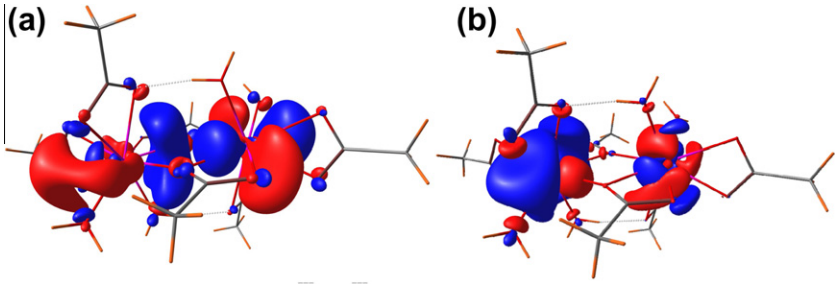

Fig. 3. NBO plots for {Gd^{III}–Gd^{III}} pair for the high spin state. (a) A donor–acceptor superimposed plot showing the donor d–p hybrid orbital of Gd^{III}(1) (left) and s–d hybrid orbital of Gd^{III}(2) (right) and (b) vice versa.

This charge transfer between the two empty orbitals of Gd(1) and Gd(2) ensures that the spin on the 4f orbitals to be aligned along the same direction. Unlike the {3d–4f} coupling where the 5d orbitals are solely involved in the charge transfer mechanism [27,28], here we observed that it is a mixture of 6s, 5d and 6p which tend to predominant the charge transfer mechanism. In this regard the mechanistic details are different than that proposed for the {3d–4f} pair. Earlier theoretical studies on the Gd^{III} dimer also emphasis the role of 5d exchanges in {4f–4f} coupling and this is also in agreement to our proposal here [42].

3.4. Magneto-structural studies

Magneto-structural correlations have been developed for complex **1** by varying the Gd–O distance, Gd–O–Gd angle and the Gd–O–Gd–O dihedral. The developed correlations are shown in Fig. 4. For Gd–O distance two different types of correlations have been attempted as the Gd–O distances in **1** is asymmetric in nature (the difference in Gd(1)–O and Gd(2)–O is 0.167 Å). The first correlation deals with the variation of Gd–O distance maintaining the asymmetry of 0.16 Å between the Gd(1)–O and Gd(2)–O distances. As the distance increases the *J* value decreases and an exponential function gives a best fit to these data points (see ESI for details). A second correlation is developed where the asymmetry parameters is varied by keeping Gd(1)–O distance constant and varying the Gd(2)–O distance. The asymmetry in the Gd–O distance has been plotted against the computed *J* values. Here, as the asymmetry increases the magnitude of the *J* decreases. However mapping the experimental points having $\{Gd_2(OAC)_2\}$ (see ESI Table S5 for details) on top of the computed points yield a poor fit revealing that

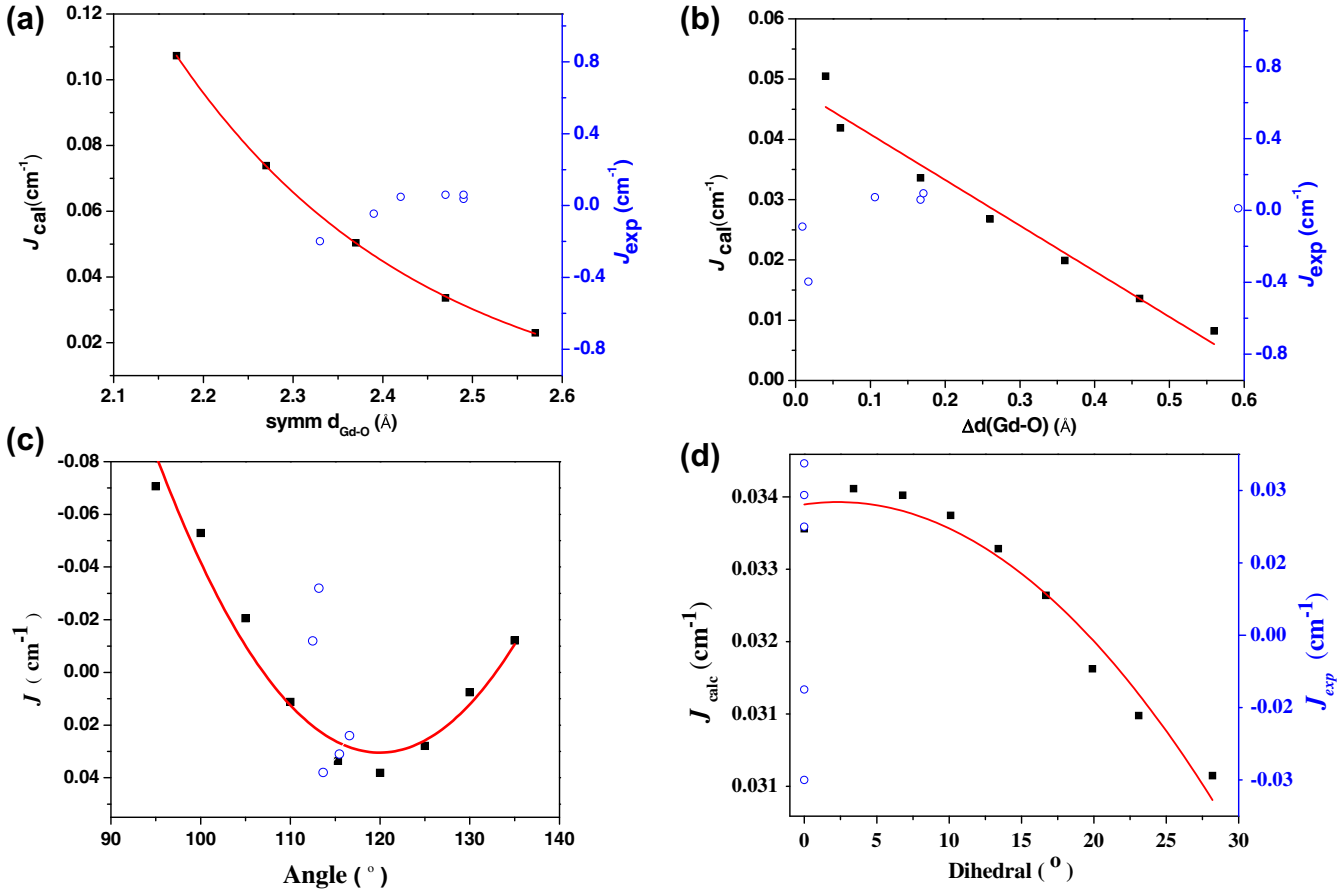

Fig. 4. Magneto-structural correlations developed by varying (a) Gd–O distances symmetrically (b) Gd–O distances asymmetrically (see text for details) (c) Gd–O–Gd bond angle and (d) Gd–O–Gd–O dihedral angle (black squares represents calculated points and blue circles represents experimental points). (Color online.)

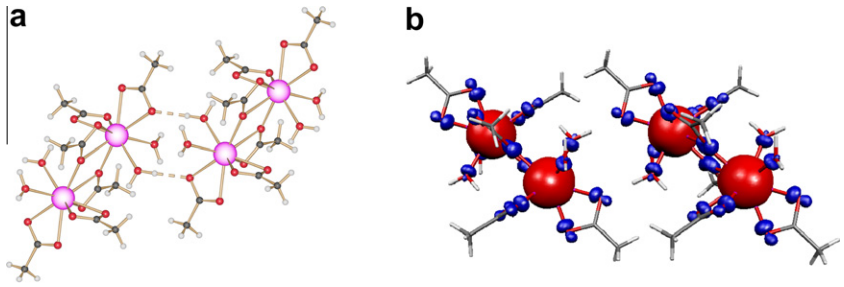

Fig. 5. The crystal structure of complex **1** reported in dimeric form connected through hydrogen bonding network. Spin density plot of dimer of dimer, where red and blue region indicates the positive and negative spin densities. (Color online.)

both these parameters are not significant in determining neither magnitude nor sign of the exchange interaction.

For angle correlation the Gd–O–Gd angle is varied from 95° to 135°. The magnetic exchange is found to follow a parabolic function with a minimum at 120° with a ferromagnetic *J* value of +0.04 cm^{-1}. Increasing or decreasing the angle from this point enhance the antiferromagnetic contribution with the *J* value becomes antiferromagnetic for angles less than ca. 106°. The spin densities on the bridging oxygens are found to follow the pattern of the computed points where a larger value of spin densities were observed for higher angle structures compared to lower angle ones (see ESI Table S3). This suggests that at higher angles electrons are rather localized leading to an increase in the ferromagnetic coupling. For the angle correlation the experimental points provide better match compared to other structural parameters.

The dihedral correlation also found to follow a parabolic function where a maximum value of *J* has been observed at a dihedral angle of *ca.* 5°. Increasing the dihedral angle further decrease the *J* values and this again is related to the increase in antiferromagnetic contribution to the net exchange. Unlike the angle parameter, there is no switch from ferro to antiferromagnetic exchange here. Moreover, plotting the experimental points on top of the computed points reveals that the dihedral parameter is not able to account for a large variation in the *J* value whereas the angle parameter is able to rationalize antiferromagnetic interaction observed in some Gd^{III} dimers [53]. From all the correlations performed above it is obvious that the Gd–O–Gd angle parameter is the most reliable parameter to address the magnetic coupling in Gd^{III} dimers. The experimental *J* value for complex **2** is found to perfectly match the computed Gd–O–Gd angle and this validates the above statement.

3.5. Exchange interaction and implication to MCE in dimer of dimer

For **1**, a large MCE has been observed due to ferromagnetic ordering at lower temperatures. This is supported by Monte Carlo simulation where a satisfactory fit to the experimental observation of the ordering temperature has been estimated [16]. Although the intermolecular interaction has not been estimated experimentally, it is clear that the sign of exchange is ferromagnetic. The crystal packing diagram of **1** reveals that, the terminal water molecule apart from participating in intramolecular hydrogen bonding also responsible for the direct intermolecular hydrogen bonding in the ab crystallographic plane. Besides there are also interplane H-bonds mediated by the additional water molecules present in the second coordination sphere [16]. To gain insight into the nature of this exchange in a dimer of dimer $\{Gd^{III}{}_2\}$ units connected via H-bonds have been constructed and exchange between two $\{Gd^{III}{}_2\}$ units have been modeled and the exchange interaction has been calculated for this model (see Fig. 5). The computed exchange is found to be ferromagnetic in nature (3×10^{-5} cm^{-1}) and this supports the experimental results [54].[2] This weak exchange due to intermolecular hydrogen bonding extend along chains in two-dimensions forming sheets and this leads to a large ground state with close lying excited states resulting in large MCE.

The computed spin density (HS) of the model is shown in Fig. 5b. The spin densities on the individual dimeric units resemble to that of the model computed above. Specifically the hydrogen and the oxygen atom of the acetates which are involved in hydrogen bonding interactions have differing spin density values suggesting that spin polarization mechanism operates to mediate this weak exchange between the dimers. Although the dipolar interactions are in the same range as the H-bond mediated intermolecular exchange, we believe that it is the H-bonding interaction which dominates here and lead to a ferromagnetic coupling and thus a ferromagnetic ordering at low temperatures. This highlights the importance of having H-bonding between molecular units to enhance the MCE.

4. Conclusion

In recent years there has been great interest in the synthesis and magnetic studies on isotropic Gd^{III} based clusters because of the possibility of achieving large MCE. Despite several experimental reports, there are only a few theoretical reports available in addressing the {4f–4f} coupling. Here, we have undertaken a comprehensive theoretical study for the first time, on a recently reported {Gd^{III}–Gd^{III}} dimer to address some important issues. The conclusions derived from this work has been summarized as follows:

(i) DFT calculations reveal that these methods are unequivocally robust in estimating exchange coupling for a {4f–4f} pair. A method assessment for {4f–4f} pair reveals that the combination of B3LYP functional along with SARC basis set on Gd^{III} with ZORA yield a best estimate of the *J* values.
(ii) The mechanistic fine details of a {4f–4f} pair has been unfolded using MO and NBO analysis where the role of 6s/5d/6p orbital in coupling has been clearly established. Besides, a major 4f–4f orbital overlaps have been detected and this essentially explains the antiferromagnetic exchange observed for some Gd^{III} dimers.
(iii) The developed magneto-structural correlations suggests that the Gd–O–Gd angle is perhaps the most important parameter which determines both the sign and magnitude of coupling in {Gd^{III}–Gd^{III}} pair.
(iv) A large MCE estimated experimentally for the studied complex stems from a ferromagnetic ordering at low temperatures. The origin of this ferromagnetic ordering is rooted

[2] The result is at the extreme limit on the accuracy of DFT calculations however such small numbers with DFT has also been reported elsewhere see for example Ref. [54].

back to ferromagnetic intermolecular interaction and our calculations clearly reveals that, it is the H-bonding interaction which essentially lead to a ferromagnetic inter-dimer coupling and underlines the importance of such intermolecular H-bonding interactions in enhancing MCE for Gd^{III} based complexes.

Further studies are underway in our laboratory to explore the {4f–4f} pair coupling further particularly on how this coupling gets affected by the presence of paramagnetic transition metal ions.

Acknowledgements

G.R. and T.R. (JRF) would like to acknowledge financial support from the Government of India through the Department of Science and Technology (SR/S1/IC-41/2010) and Indian Institute of Technology, Bombay for a JRF (S.K.S.) position and access to high performance computing facility.

Appendix A. Supplementary data

Supplementary data associated with this article can be found, in the online version, at http://dx.doi.org/10.1016/j.poly.2012.06.017.

References

[1] (a) R. Sessoli, D. Gatteschi, A. Caneschi, M.A. Novak, Nature 365 (1993) 141;
(b) G. Christou, D. Gatteschi, D.N. Hendrickson, R. Sessoli, Mater. Res. Bull. 25 (2000) 66;
(c) D. Gatteschi, R. Sessoli, J. Villain, Molecular Nanomagnets, Oxford University Press, Oxford, 2006.
[2] R. Sessoli, H.-L. Tsai, A.R. Schake, S. Wang, J.B. Vincent, K. Folting, D. Gatteschi, G. Christou, D.N. Hendrickson, J. Am. Chem. Soc. 115 (1993) 1804.
[3] (a) S. Sanvito, Chem. Soc. Rev. 40 (2011) 3336;
(b) L. Bogani, W. Wersdorfer, Nat. Mater. 7 (2008) 179;
(c) B. Fleury, L. Catala, V. Huc, C. David, W.Z. Zhong, P. Jegou, L. Baraton, S. Palacin, P.A. Albouy, T. Mallah, Chem. Commun. (2005) 2020.
[4] (a) M. Leuenberger, D. Loss, Nature 410 (2001) 6830;
(b) S. Hill, R.S. Edwards, N. Alliaga-Alcalde, G. Christou, Science 302 (2003) 1015;
(c) M. Affronte, F. Troiani, A. Ghirri, A. Candini, M. Evangelisti, V. Corradini, S. Carretta, P. Santini, G. Amoretti, F. Tuna, G. Timco, R.E.P. Winpenny, J. Phys. D., Appl. Phys. 40 (2007) 2999;
(d) F.K. Larsen, E.J.L. McInnes, H.El. Mkami, J. Overgaard, S. Piligkos, G. Rajaraman, E. Rentschler, A.A. Smith, G.M. Smith, V. Boote, M. Jennings, G. A Timco, R.E.P. Winpenny, Angew. Chem., Int. Ed. 42 (2003) 101;
(e) F. Troiani, A. Ghirri, M. Affronte, S. Carretta, P. Santini, G. Amoretti, S. Piligkos, G. Timco, R.E.P. Winpenny, Phys. Rev. Lett. 94 (2005) 207208.
[5] S.-D. Jiang, B.-W. Wang, G. Su, Z.-M. Wang, S. Gao, Angew. Chem., Int. Ed. 49 (2010) 7448.
[6] N. Ishikawa, M. Sugita, T. Ishikawa, S.-Y. Koshihara, Y. Kaizu, J. Phys. Chem. B 108 (2004) 11265.
[7] N. Zhou, Y. Ma, C. Wang, G.Xu. Feng, J.-K. Tang, J.-X. Xu, S.-P. Yan, D.-Z. Liao, Dalton Trans. (2009) 8489.
[8] (a) L. Bogani, A. Vindigni, R. Sessoli, D. Gatteschi, J. Mater. Chem. 18 (2008) 4750;
(b) K. Bernot, L. Bogani, A. Caneshi, D. Gatteschi, R. Sessoli, J. Am. Chem. Soc. 128 (2006) 7947;
(c) R.J. Glauber, J. Math. Phys. 4 (1963) 294;
(d) H. Miyasaka, M. Julve, M. Yamashita, R. Clerac, Inorg. Chem. 48 (2009) 3420;
(e) A.R. Rocha, V.M.G. Suarez, S.W. Bailey, C.J. Lambert, J. Ferrer, S. Sanvito, Nat. Mater. 4 (2005) 335.
[9] (a) M.A. AlDamen, J.M. Clemente-Juan, E. Coronado, C. Mari-Gastaldo, A. Gaito-Arina, J. Am. Chem. Soc. 130 (2008) 8874;
(b) N. Ishikawa, J. Phys. Chem. A 107 (2003) 5831;
(c) N. Ishikawa, M. Sugita, T. Ishikawa, S.Y. Koshihara, Y. Kaizu, J. Am. Chem. Soc. 125 (2003) 8694;
(d) N. Ishikawa, M. Sugita, W. Wernsdorfer, J. Am. Chem. Soc. 127 (2005) 3650.
[10] (a) O. Waldmann, J. Hassmann, P. Müller, G.S. Hanan, D. Volkmer, U.S. Schubert, J.-M. Lehn, Phys. Rev. Lett. 78 (1997) 3390;
(b) O. Cador, D. Gatteschi, R. Sessoli, F.K. Larsen, J. Overgaard, A.-L. Barra, S.J. Teat, G.A. Timco, R.E.P. Winpenny, Angew. Chem., Int. Ed. 43 (2004) 5196.
[11] (a) P.-H. Lin, T.J. Burchell, L. Ungur, L.F. Chibotaru, W. Wernsdorfer, M. Murugesu, Angew. Chem., Int. Ed. 48 (2009) 9489;
(b) R.J. Blagg, C.A. Muryn, E.J.L. McInnes, F. Tuna, R.E.P. Winpenny, Angew. Chem., Int. Ed. 50 (2011) 6530;
(c) B. Hussain, D. Savard, T.J. Burchell, W. Wernsdorfer, M. Murugesu, Chem. Commun. (2009) 1100.
[12] (a) Yu.I. Spichkin, A.K. Zvezdin, S.P. Gubin, A.S. Mischenko, A.M. Tishin, J. Phys. D 34 (2001) 1162;
(b) F. Torres, J.M. Hernndez, X. Bohigas, J. Tejada, Appl. Phys. Lett. 77 (2000) 3248;
(d) F. Torres, X. Bohigas, J.M. Hernndez, J. Tejada, J. Phys. Condens. Matter 15 (2003) L119;
(e) M. Affronte, A. Ghirri, S. Carretta, G. Amoretti, S. Piligkos, G.A. Timco, R.E.P. Winpenny, Appl. Phys. Lett. 84 (2004) 3468;
(f) J. Schnack, R. Schmidt, J. Richter, Phys. Rev. B 76 (2007) 054413.
[13] T. Feder, Phys. Today 62 (2009) 21.
[14] (a) C. Zimm, A. Jastrab, A. Sternberg, V.K. Pecharsky Jr., K. Gschneidner, M. Osborne, I. Anderson, Adv. Cryog. Eng. 43 (1998) 1759;
(b) V.K. Pecharsky Jr., K.A. Gschneidner, J. Magn. Magn. Mater. 200 (1999) 44;
(c) K.A. Gschneidner Jr., V. Pecharsky, Int. J. Refrig. 31 (2008) 945.
[15] M. Manoli, R.D.L. Johnstone, S. Parsons, M. Murrie, M. Affronte, M. Evangelisti, E.K. Brechin, Angew. Chem., Int. Ed. 46 (2007) 4456.
[16] (a) M. Evangelisti, O. Roubeau, E. Palacios, A. Camon, T.N. Hooper, E.K. Brechin, J.J. Alonso, Angew. Chem., Int. Ed. 50 (2011) 6606;
(b) S.T. Hatscher, W. Urland, Angew. Chem., Int. Ed. 42 (2003) 2862;
(c) J.W. Sharples, Y.-Z. Zheng, F. Tuna, E.J.L. McInnes, D. Collison, Chem. Commun. 47 (2011) 7650;
(d) S.K. Langley, N.F. Chilton, B. Moubaraki, T. Hooper, E.K. Brechin, M. Evanghelisti, K.S. Murray, Chem. Sci. 2 (2011) 1166.
[17] G. Karotsis, S. Kennedy, S.J. Teat, C.M. Beavers, D.A. Fowler, J.J. Morales, M. Evangelisti, S.J. Dalgarno, E.K. Brechin, J. Am. Chem. Soc. 132 (2010) 12983.
[18] M. Evangelisti, O. Roubeau, E. Palacios, A. Camon, T.N. Hooper, E.K. Brechin, J.J. Alonso, Angew. Chem., Int. Ed. 50 (2011) 6606.
[19] Y.-Z. Zheng, M. Evangelisti, R.E.P. Winpenny, Angew. Chem., Int. Ed. 50 (2011) 3692.
[20] Y.-Z. Zheng, E.M. Pineda, M. Helliwell, R.E.P. Winpenny, Chem. Eur. J. 18 (2012) 4161.
[21] A.S. Dinca, A. Ghirri, A.M. Madalan, M. Affronte, M. Andruh, Inorg. Chem. 51 (2012) 3935.
[22] a) M. Evangelisti, E.K. Brechin, Dalton Trans. 39 (2010) 4672;
b) F.-S. Guo, J.-D. Leng, J.-L. Liu, Z.-S. Meng, M.-L. Tong, Inorg. Chem. 51 (2012) 405.
[23] E. Ruiz, S. Alvarez, A. Rodriguez-Fortea, P. Alemany, Y. Pouillon, C. Massobrio, in: J.S. Miller, M. Drillon (Eds.), Magnetism: Molecules to Materials, vol. II, Wiley-VCH, Weinheim, 2001, p. 227.
[24] S. Piligkos, G. Rajaraman, M. Soler, N. Kirchner, J. van Slageren, R. Bircher, S. Parsons, H. Guedel, J. Kortus, W. Wernsdorfer, G. Christou, E.K. Brechin, J. Am. Chem. Soc. 127 (2005) 5572.
[25] G. Rajaraman, M. Murugesu, E.C. Sanudo, M. Soler, W. Wernsdorfer, M. Helliwell, C. Muryn, J. Raftery, S.J. Teat, G. Christou, E.K. Brechin, J. Am. Chem. Soc. 126 (2004) 15445.
[26] A. Bencini, F. Totti, Int. J. Quantum Chem. 6 (2005) 819.
[27] (a) G. Rajaraman, F. Totti, A. Bencini, A. Caneschi, R. Sessoli, D. Gatteschi, Dalton Trans. (2009) 3153;
(b) S.K. Singh, N.K. Tibrewal, G. Rajaraman, Dalton Trans. 40 (2011) 10897.
[28] J. Cirera, E. Ruiz, C. R. Chimie 11 (2008) 1227.
[29] L. Canadillas-Delgado, O. Fabelo, J. Cano, J. Pasan, F.S. Delgado, F. Lloret, M. Julve, C. Ruiz-Perez, CrystEngComm 11 (2009) 2131.
[30] L. Noodleman, J. Chem. Phys. 74 (1981) 5737.
[31] (a) E. Ruiz, S. Alvarez, J. Cano, P. Alemany, J. Comput. Chem. 20 (1999) 1391;
(b) E. Ruiz, A.R. Fortea, J. Cano, S. Alvarez, P. Alemany, J. Comput. Chem. 24 (2003) 982;
E. Ruiz, J. Cano, S. Alvarez, A. Caneschi, D. Gatteschi, J. Am. Chem. Soc. 152 (2003) 6791;
(d) G. Rajaraman, J. Cano, E.K. Brechin, E.J.L. McInnes, Chem. Commun. (2004) 1476.
[32] M.J. Frisch, G.W. Trucks, H.B. Schlegel, G.E. Scuseria, M.A. Robb, J.R. Cheeseman, G. Scalmani, V. Barone, B. Mennucci, G.A. Petersson, H. Nakatsuji, M. Caricato, X. Li, H.P. Hratchian, A.F. Izmaylov, J. Bloino, G. Zheng, J.L. Sonnenberg, M. Hada, M. Ehara, K. Toyota, R. Fukuda, J. Hasegawa, M. Ishida, T. Nakajima, Y. Honda, O. Kitao, H. Nakai, T. Vreven, J.A. Montgomery Jr., J.E. Peralta, F. Ogliaro, M. Bearpark, J.J. Heyd, E. Brothers, K.N. Kudin, V.N. Staroverov, R. Kobayashi, J. Normand, K. Raghavachari, A. Rendell, J.C. Burant, S.S. Iyengar, J. Tomasi, M. Cossi, N. Rega, J.M. Millam, M. Klene, J.E. Knox, J.B. Cross, V. Bakken, C. Adamo, J. Jaramillo, R. Gomperts, R.E. Stratmann, O. Yazyev, A.J. Austin, R. Cammi, C. Pomelli, J.W. Ochterski, R.L. Martin, K. Morokuma, V.G. Zakrzewski, G.A. Voth, P. Salvador, J.J. Dannenberg, S. Dapprich, A.D. Daniels, Ö. Farkas, J.B. Foresman, J.V. Ortiz, J. Cioslowski, D.J. Fox, Gaussian 09, Revision A.1, Gaussian Inc., Wallingford, CT, 2009.
[33] A.D. Becke, J. Chem. Phys. 98 (1993) 5648.
[34] T.R. Cundari, W.J. Stevens, J. Chem. Phys. 98 (1993) 5555.
[35] Orca, 2.6.2360, F. Neese, Bonn, 2010.
[36] D.A. Pantazis, F. Neese, J. Chem. Theory Comput. 5 (2009) 2229.
[37] A. Schafer, C. Huber, R. Ahlrichs, J. Chem. Phys. 100 (1994) 5829.
[38] B.A. Hess, Phys. Rev. A 32 (1985) 756.
[39] E.V. Lenthe, E.J. Baerends, J.G. Snijders, J. Chem. Phys. 99 (1993) 4597.
[40] M. Douglas, N.M. Kroll, Ann. Phys. 82 (1974) 89.
[41] a) G.B. Kauffman, Adv. Chem. 62 (1967) 41;
b) A. Werner, Z. Anorg. Allg. Chem. 2 (1893) 267;

(c) G.B. Kauffman, Classics in Coordination Chemistry, Part 1: The Selected Papers of A. Werner, Dover, New York, 1968. pp. 9.
[42] (a) L.E. Sweet, L.E. Roy, F. Meng, T. Hughbanks, J. Am. Chem. Soc. 128 (2006) 10193;
(b) L.E. Roy, T. Hughbanks, J. Am. Chem. Soc. 128 (2006) 568.
[43] (a) L. Zhu, K.L. Yao, Z.L. Liu, Phys. Rev. B 76 (2007) 134409;
(b) S.C. Manna, E. Zangrando, A. Bencini, C. Benelli, N.R. Chaudhuri, Inorg. Chem. 45 (2006) 9114;
(c) L. Canadillas-Delgado, J. Cano, O. Fabelo, C. Ruiz-Perez, Gadolinium Compound: Production and Applications, Nova Publisher, 2010, pp. 1.
[44] F. Yan, Z.D. Chen, J. Phys. Chem. A 104 (2000) 6295.
[45] S. Gao, O. Borgmeier, H. Lueken, Acta Phys. Pol. A 90 (1996) 393.
[46] X. Xu, W.A. Goddard III, Proc. Natl. Acad. Sci. 101 (2004) 2673.
[47] B. Miehlich, A. Savin, H. Stoll, H. Preuss, Chem. Phys. Lett. 157 (1989) 200; A.D. Becke, Phys. Rev. A 38 (1988) 3908.
[48] J.P. Perdew, Phys. Rev. B 33 (1986) 8822.
[49] A.D. Becke, Phys. Rev. A 38 (1988) 3908.
[50] J.M. Tao, J.P. Perdew, V.N. Staroverov, G.E. Scuseria, Phys. Rev. Lett. 91 (2003) 146401.
[51] (a) O. Kahn, B. Briat, J. Chem. Soc., Faraday Trans. 2 72 (1976) 268;
(b) O. Kahn, B. Briat, J. Chem. Soc., Faraday Trans. 2 72 (1976) 1441.
[52] C. Kollmar, O. Kahn, J. Chem. Phys. 96 (1992) 2988.
[53] L. Canadillas-Delgado, O. Fabelo, J. Pasan, F.S. Delgado, F. Lloret, M. Julveb, C. Ruiz-Perez, Dalton Trans. 39 (2010) 7286.
[54] S. Gomez-Coca, E. Ruiz, J. Kortus, Chem. Commun. (2009) 4363.
[55] E. Ruiz, J. Cano, S. Alvarez, P. Alemany, J. Am. Chem. Soc. 120 (1998) 11122.